Experimental Neurology 316 (2019) 27–38

Contents lists available at ScienceDirect

Experimental Neurology

journal homepage: www.elsevier.com/locate/yexnr

Research Paper

Excess glutamate secreted from astrocytes drives upregulation of P-glycoprotein in endothelial cells in amyotrophic lateral sclerosis

Loqman A. Mohamed, Shashirekha S. Markandaiah, Silvia Bonanno, Piera Pasinelli, Davide Trotti*

Jefferson Weinberg ALS Center, Vickie and Jack Farber Institute for Neuroscience, Department of Neuroscience, Thomas Jefferson University, 900 Walnut Street, Philadelphia, PA 19107, USA

ARTICLE INFO

Keywords:
Amyotrophic lateral sclerosis
Blood brain barrier
P-glycoprotein
Pharmacoresistance
Glutamate
Endothelial cells
Riluzole
NMDA receptor

ABSTRACT

In amyotrophic lateral sclerosis (ALS), upregulation in expression and activity of the ABC transporter P-glycoprotein (P-gp) driven by disease advancement progressively reduces CNS penetration and efficacy of the ALS drug, riluzole. Post-mortem spinal cord tissues from ALS patients revealed elevated P-gp expression levels in endothelial cells of the blood-spinal cord barrier compared to levels measured in control, non-diseased individuals. We recently found that astrocytes expressing familial ALS-linked SOD1 mutations regulate expression levels of P-gp in endothelial cells, which also exhibit a concomitant, significant increase in reactive oxygen species production and NFκB nuclear translocation when exposed to mutant SOD1 astrocyte conditioned media. In this study, we found that glutamate, which is abnormally secreted by mutant SOD1 and sporadic ALS astrocytes, drives upregulation of P-gp expression and activity levels in endothelial cells *via* activation of N-Methyl-D-Aspartic acid (NMDA) receptors. Surprisingly, astrocyte-secreted glutamate regulation of endothelial P-gp levels is not a mechanism shared by all forms of ALS. C9orf72-ALS astrocytes had no effect on endothelial cell P-gp expression and did not display increased glutamate secretion. Utilizing an optimized *in vitro* human BBB model consisting of patient-derived induced pluripotent stem cells, we showed that co-culture of endothelial cells with patient-derived astrocytes increased P-gp expression levels and transport activity, which was significantly reduced when endothelial cells were incubated with the NMDAR antagonist, MK801. Overall, our findings unraveled a complex molecular interplay between astrocytes of different ALS genotypes and endothelial cells potentially occurring in disease that could differentially impact ALS prognosis and efficacy of pharmacotherapies.

1. Introduction

Amyotrophic lateral sclerosis (ALS) is a progressive, invariably fatal, neurodegenerative disease. Like for many other neurodegenerative diseases, ALS complex pathogenesis is under intense investigation facilitated by the discovery of the many disease-causative genetic mutations (Hardiman et al., 2017; Katyal and Govindarajan, 2017). Nevertheless, ALS currently remains an incurable disease; therefore, finding effective therapeutic agents is still a pressing necessity.

One of the requirements for bioactive drugs to reach their site of action in the CNS is the ability to cross the blood brain barrier (BBB), a protective barrier that separates the blood constituents from the CNS parenchyma (Qosa et al., 2016b). Although the BBB is essential to maintain brain nutrients homeostasis and protects the CNS from potentially harmful xenobiotics, it is an obstacle to brain penetration in effective therapeutic concentrations for most drugs to reach the brain (Abbott, 2013; Qosa et al., 2016b). The BBB is essentially composed of endothelial cells held together by tight junctions and supported by other brain structures such as the basal lamina and cells such as pericytes and astrocytes that regulate BBB properties (Abbott and Friedman, 2012). One important molecular determinant of the BBB is P-glycoprotein (P-gp), a major multidrug efflux transporter protein

Abbreviations: ALS, amyotrophic lateral sclerosis; ACM, astrocyte conditioned medium; BBB, blood brain barrier; COX2, cyclooxygenase type 2; ECs, endothelial cells; EP-I, prostaglandin E2 receptor 1; ECF, extracellular fluid; MDR1, multidrug resistance protein-1; MRPs, multidrug receptor-associated proteins; NMDAR, *N*-methyl-D-aspartic acid receptor; NFkB, nuclear factor kappa-light-chain-enhancer of activated B cells; P-gp, permeability glycoprotein or P-glycoprotein; PLA2, phospholipase A2; TEER, trans-endothelial electrical resistance; Nrf2, nuclear factor erythroid-2 related factor; ROS, reactive oxygen species

* Corresponding author.
E-mail address: davide.trotti@jefferson.edu (D. Trotti).

https://doi.org/10.1016/j.expneurol.2019.04.002
Received 29 November 2018; Received in revised form 9 March 2019; Accepted 6 April 2019
Available online 09 April 2019
0014-4886/

expressed at the blood side of the microcapillary endothelium (Qosa et al., 2015). P-gp acts as an efflux pump that transport its substrates into the blood stream, preventing accumulation of many drugs into the CNS. In many neurologic disorders, including ALS, the expression of P-gp at the BBB is upregulated, which makes the net penetration of CNS therapeutics to the brain even more of a challenging task (Jablonski et al., 2012; Loscher et al., 2011). P-gp expression at the BBB is controlled by multiple receptor–mediated signaling pathways that are themselves regulated by several cell stressors, neurotransmitters, as well as inflammatory mediators, which are usually subjected to drastic changes in neurologic disorders (Qosa et al., 2015). For example, ischemia and tissue hypoxia in stroke gives rise to pro-inflammatory mediators and reactive oxygen species (ROS), which were shown to increase P-gp expression levels and function *via* NFκB nuclear translocation (Felix and Barrand, 2002; Miller et al., 2008). We identified a similar pathway that engages ROS production and activation of NFκB nuclear translocation in P-gp upregulation in spinal cord and cerebral capillaries of SOD1-G93A mice models of ALS as well as in human iPS-derived ECs cultured with mutant SOD1 astrocytes (Qosa et al., 2016a). The close proximity of the astrocyte end feet makes astrocytes a major contributor to the regulation and maintenance of the BBB phenotype (Abbott et al., 2010). Several studies have demonstrated the role of astrocytes in regulating P-gp expression and tight junction formation by the capillary endothelium of the BBB, and hence, pathologic changes in astrocytes may negatively impact their BBB regulatory function (Baello et al., 2016; Qosa et al., 2015).

In this work, we further our investigation on the mechanisms that drive upregulation of P-gp at the capillary endothelium in ALS attributed to astrocytes secreted soluble factors. In ALS, astrocytes are unable to efficiently reuptake glutamate in the synapses and, thus allow elevated glutamate levels in the brain's extracellular fluid (ECF) to develop glutamate-mediated excitotoxicity *via* activation of glutamate receptors and neuroinflammation (Rosenblum and Trotti, 2017). High ECF glutamate increases P-gp expression at the BBB in epilepsy, which led to reduction in brain penetration of anti-epileptic drugs (Potschka, 2010). Thus, we postulated that the abnormally high extracellular glutamate levels in ALS may induce P-gp over-expression at the capillary endothelium of the BBB. We found that astrocytes in culture derived from sporadic or SOD1-A4V, but not C9orf72 ALS patients, abnormally allow for elevated levels of glutamate in the medium. Short and long-term exposure of ECs to astrocyte conditioned medium (ACM) upregulated P-gp expression levels and function by glutamate-mediate activation of the NMDARs and cyclooxygenase-II (COX2), events that are upstream to NFκB nuclear translocation and P-gp upregulation.

2. Materials and methods

2.1. Chemicals

Human iPS-derived endothelial cells were purchased from Cellular Dynamics (Cat# ECM-100-030-001; from healthy donor). Dulbecco's modified Eagle's medium (DMEM) was purchased from Invitrogen (Carlsbad, CA). Bovine (BSA) and fetal bovine sera (FBS) were purchased from Sigma-Aldrich (St. Louis, MO). The reagents and supplements required for western blotting were purchased from Bio-Rad (Hercules, CA). Total protein measurement's reagents with the bicinchoninic acid (BCA) method were obtained from Pierce (Rockford, IL). All other chemicals and reagents were of analytical grade and were readily available from commercial sources.

2.2. Animals

Brains of 3–4 months old Sprague Dawley rats (Charles River, strain #400) were used for the isolation of microcapillaries using an equal ration of male:female brains. Rats were allowed easy access to water and food, and housed at 22 °C, 35% relative humidity and 12 h dark/light cycle. All experiments involving animals were approved by the Institutional Animal Care and Use Committee (IACUC) of Thomas Jefferson University and all surgical procedures were consistent with the IACUC policies and procedures.

2.3. Cell cultures

Astrocytes were differentiated from human induced pluripotent stem cells (iPSCs) derived from ALS patients of either SOD1-A4V, sporadic (procured by Dr. Nicholas Maragakis, Johns Hopkins University), or C9orf72 (Target ALS) genotype, and normal (non-ALS) human subjects (Control) (Cellular Dynamic, Cat. #R1092) (Boulting et al., 2011; Frakes et al., 2014b). Human iPS-derived astrocytes (two lines for control and for ALS genotype) were plated in 75T flasks pre-coated with 1% matrigel, cultured in 1:1 DMEM/F12 medium (supplemented with 1% fetal bovine serum (FBS), 1% *w/v* nonessential amino acids, L-glutamine 2 mM, Heparin (2 mg/mL), 2% B27, and the antibiotics penicillin G (100 units/mL) and streptomycin (100 μg/mL), and used at DIV 90–100 when astrocytes robustly express markers characteristic of the astrocytic phenotype, such as GFAP, S100β and the glutamate transporter EAAT1 (Haidet-Phillips et al., 2014). Human iPS-derived ECs (Cellular Dynamics, Cat# ECM-100-030-001), were plated in T-75 flasks pre-coated with 30 μg/mL fibronectin, and cultured in VascuLife basal medium (Lifeline cell technology, MD) supplemented with 5 ng/mL rh FGF basic, 50 mg/mL ascorbic acid, 1 mg/mL hydrocortisone sulfate, 10 mM L-glutamine, 15 ng/mL rh IGF-1, 5 ng/mL rh EGF, 5 ng/mL rh VEGF, 0.75 IU/mL heparin sulfate, penicillin G (100 IU/mL), streptomycin (100 μg/mL), and 10% iCell endothelial cells medium supplement (Cellular Dynamics).

2.4. Treatment with astrocyte-conditioned media

Human iPS-derived astrocytes were allowed to reach ~80% confluency at which point culture medium was replaced with fresh medium and the cells further cultured for 72 h. Astrocyte conditioned media (ACM) were collected at this DIV from three cultures (SOD1-A4V, sporadic, and control) centrifuged at 1000 rpm for 5 min to remove debris and floating cells, and stored in aliquots at −80 °C. Human iPS-derived ECs were cultured in 24-well plates to reach ~80% confluency, then the cells were treated with 0.5 mL of ACM for 30 min. ACM was completely replaced with glutamate-free medium and cells were further kept in culture for additional 24 h. For inhibition studies, cells were pre-treated for 15 min with inhibitors (1 μM MK801, 5H-dibenzo[*a*,*d*]cyclohepten-5,10-imine (dizocilpine maleate), a non-competitive antagonist of the glutamate receptor N-Methyl-D-Aspartate receptor (NMDA), 1 μM celecoxib, a selective cycloxygenase-2 (COX-2) antagonist). The inhibitors were further added during the ACM incubation period of for 30 min.

2.5. Brain capillary isolation

Freshly isolated rat brain hemispheres were cleared from the meninges and choroid plexus and immediately homogenized in ice-cold D-PBS (2.7 mM KCl, 1.46 mM KH_2PO_4, 136.9 mM NaCl, 8.1 mM Na_2HPO_4, 0.9 mM $CaCl_2$, and 0.5 mM $MgCl_2$ supplemented with 5 mM D-glucose, 1 mM sodium pyruvate, pH 7.4), containing a protease inhibitor cocktail (Cat. #78438, Thermoscientific). Brain capillaries (microvessels) were isolated as described previously with some modifications (Mohamed et al., 2016; Qosa et al., 2016a). Briefly, after homogenization of brain hemispheres in D-PBS, the homogenate was mixed 1:1 with 30% Ficoll and centrifuged at 5800 ×*g* for 15 min at 4 °C. Supernatant was discarded and pellet containing microvessels was gently resuspended in ice-cold D-PBS containing 1% BSA and passed through a column packed with glass beads. Microvessels adhered to the glass beads were collected by gentle shaking into BSA-free D-PBS followed by centrifugation at 5800 ×*g* for 5 min at 4 °C. Pelleted

microvessels of both brain and spinal cord were separately mixed with 2% matrigel containing media, incubated in a humidified atmosphere (5% CO_2/95% air) at 37 °C for 1 h and used immediately for P-gp transport activity studies, as described below.

2.6. P-glycoprotein transport activity

2.6.1. In vitro permeability studies

Human iPS-derived astrocytes (from normal or ALS subjects) were cultured in 24-well plates. Human iPS-derived ECs were grown as monolayers by culturing the cells (50,000 cells/cm^2) on 24-transwell polyester membrane inserts (0.4 μm pores; Corning, NY) pre-coated with 60 μg/mL of fibronectin solution prepared in distilled water. After 2 days of culture, inserts then were placed on top of the astrocyte layer and incubated for 72 h at 37 °C. Human iPS-derived ECs were used between passages 2 and 5 (Lippmann et al., 2014). Another set of iPS-derived ECs, to be used for ACM treatment, were cultured alone on inserts for 6 days until they form a continuous monolayer. Subsequently, cells were treated with ACM from either iPS-derived astrocytes from ALS patients of different genotypes or normal subject for 30 min followed by replacement with fresh medium and further cultured for 5.5 h. For NMDA receptor inhibition, cells were treated with MK801 (1 μM) for 15 min before addition of ACM and during its incubation for 30 min. Subsequently, EC monolayers either from co-culture or ACM-treated cells were used for P-gp transport assays. Endothelial cell monolayers on inserts were treated for 60 min with LD800 (50 μM), a P-gp fluorescent specific substrate, and NaF (50 μM), a paracellular permeability marker, dissolved in culture media. The aforementioned treatments were applied to the basolateral side (B, lower chamber, representative of the brain side) to initiate basolateral to apical (A, upper chamber, representative of blood side) transport (B → A). At the end of treatment, transport was ended by separation of inserts from their wells and aliquots were taken from both apical and basolateral sides for analysis. Transport quotient (TQ) of LD800 from B → A was calculated using the following equation:

$$LD800\ TQ = \frac{(LD800\ (\text{apical}))/(LD800\ (\text{total}))}{(NaF\ (\text{apical}))/(NaF\ (\text{total}))} \quad (1)$$

where LD800 $_{(\text{total})}$ is the sum of LD800 in the apical and basolateral compartments, and NaF $_{(\text{total})}$ is the sum of NaF in the apical and basolateral compartments.

2.6.2. Isolated capillary transport assay

To assess P-gp function in isolated brain capillaries, we used a confocal microscopy-based transport assay, which have been described previously (Hartz et al., 2004; Jablonski et al., 2012). Isolated capillaries were placed on cover-slips coated with 2% matrigel, which was placed on glass slides at the end of transport experiment for microscopic analysis. First, isolated capillaries were exposed for 30 min to ACM/SOD1-A4V or ACM/sporadic, then replaced with fresh media and incubated for additional 5.5 h. For inhibition studies, isolated capillaries were pretreated for 15 min with inhibitors (1 μM MK801 or 1 μM celecoxib), then ACM was added together with the inhibitor for the designated time period mentioned earlier. Subsequently, transport assay was initiated by incubating capillaries with fluorescent P-gp substrate, NBD-CSA, and luminal substrate accumulation was measured 1 h later. To acquire images, the slides containing capillaries were mounted on the stage of an inverted Olympus Fluoview 1000 Confocal laser scanning microscope (Olympus, PA) and imaged using a × 40 objective and a 488-nm laser line for NBD-CSA. Captured images were analyzed for the luminal accumulation of the fluorescence NBD-CSA by Image J software (NIH, Bethesda, MD, USA). Data are presented as arbitrary fluorescence units from 6 to 8 images.

2.6.3. Western blot analysis

Spinal cord autopsy samples from control and ALS patients (sporadic, SOD1-AV4 and C9orf72; Target ALS tissue sample ID: #103 Control, #90 sporadic, #43 SOD1, #16 C9orf72) were obtained from Target ALS tissue bank. Spinal cord tissue (~100 mg) was homogenized in 1 mL of RIPA buffer in the presence of protease inhibitor cocktail (Cat. #78438,Thermoscientific), centrifuged at 1000 × *g* for 10 min at room temperature and the supernatant was used to prepare the samples for Western blot analysis. 25 μg of total protein for each sample group were run on 4–12% stain-free gel (Bio-rad) and transferred to a nitrocellulose membrane using turbo-blot semi transfer system (Bio-rad). The membrane was blocked with 5% BSA in PBST for an hour at room temperature followed by incubation with primary antibodies overnight, followed by incubation with corresponding secondary antibodies conjugated to horseradish peroxidase (1 h, room temperature). Membrane was developed by chemiluminescence and bands were visualized using a Chemidoc™ one touch system (BIO-RAD; Hercules, CA), and quantified by densitometric analysis.

Human iPS-derived endothelial cells were collected in 1.5 mL Eppendorf tubes and centrifuged at 2000 *g* for 10 min at 4 °C. Cells were then lysed in RIPA buffer containing protease inhibitors cocktail. Supernatants were stored at −80 °C for subsequent western blot analyses. Next, 25 μg of protein samples was loaded 5% SDS-polyacrylamide gel cassette and resolved at 140 V for 1.5 h and transferred electrophoretically onto nitrocellulose membranes at 300 mA for 3 h. Membranes were blocked with 2% BSA blocking solution prepared in PBS for 1 h at room temperature, followed by addition of primary mouse monoclonal antibodies for P-gp (BioLegend Cat# 901401, clone C-219, 1:50 dilution, RRID:AB_2565004) and GAPDH (Fitzgerald 1:20,000 dilution; Cat# 10R-G109a, RRID:AB_1285808), and incubated overnight at 4 °C. Membranes then washed three times and incubated into secondary antibodies; horseradish peroxidase (HRP) labeled anti-mouse IgG antibody for P-gp and GAPDH. Protein blots were developed using a chemiluminescence detection kit (SuperSignal West Femto substrate; Thermo Scientific, Waltham, MA). Bands were visualized using a Bio-Rad chemidoc TM one touch system (BIO-RAD; Hercules, CA), and quantified by densitometric analysis.

2.6.4. Immunocytochemistry

Cells were washed with PBS twice and fixed for 10 min in PBS solution containing 4% paraformaldehyde and 4% sucrose, and permeabilized with 0.25% triton-100× for another 10 min at room temperature. After washing 3 times with PBS, cells were blocked with 10% horse serum for 1 h at room temperature. Next, cells were incubated overnight at 4 °C with primary antibodies prepared in 10% blocking solution containing 0.1% tween-20. Primary antibodies used including mouse monoclonal P-gp antibody C219 (Covance; MA) at 1:50 dilution, and rabbit monoclonal NFκB antibody (Abcam, MA) at 1:100 dilution. Subsequently cells were washed three times with PBS and incubated for 1 h at room temperature with secondary antibodies either Alexa Fluor 488 donkey anti-mouse IgG (Thermo Fisher Scientific Cat# R37114, RRID:AB_2556542) or Alexa Fluor 546 donkey anti-rabbit IgG (Thermo Fisher Scientific Cat# A10040, RRID:AB_2534016) at 1:200 dilutions followed by washing cells three times with PBS. Transwell membranes were collected and mounted with Prolong Gold DAPI antifade solution (Life technologies, CA) and images were captured using Olympus Fluoview 1000 Confocal laser scanning microscope (Olympus, PA) at a total magnification of 400×. Total signal of P-gp was quantified using NIH ImageJ version 1.44 software as described previously (Noursadeghi et al., 2008).

2.6.5. Glutamate release measurement in cell culture

Glutamate level in ACM from either human iPS astrocytes derived from the control subject or ALS patients (Sporadic and familial) were measured using Amplex Red Glutamic acid assay kit (Invitrogen). According to manufacturer instructions, glutamate levels in ACM were measured fluoremetrically using BMG LABTECH POLARstar-plate reader (BMG LABTECH Inc., NC). Data were normalized to protein

content and converted to concentration by comparison to standard glutamate solution.

2.6.6. Fluorescence spectrophotometric measurement of [Ca^{2+}] in iPS endothelial cells treated with astrocyte conditioned media (ACM)

Intracellular level of calcium was monitored by measuring the change in the fluorescence intensity of Fluo-4-loaded cells (Johnson et al., 2002). First, human iPS-derived endothelial cells was cultured on 96-well plates and allowed to reach confluence. Then, cells were treated with 200 µl of standard HBSS buffer containing 2.5 µM Fluo-4, AM and Pluronic F-27 and incubated in the dark for 1 h at 37 °C. Subsequently, cells were washed three times with HBSS and incubated for another 2 h in media. Calcium response was measured by monitoring a baseline fluorescence of cells loaded with Fluo-4, AM alone for 5 min, followed by addition of ACM alone or with NMDA receptor antagonist, 5 µM MK801 and measurement was continued for 45 min at 37 °C. Fluorescence was measured in a plate spectrofluorimeter, BMG LABTECH POLARstar-plate reader (BMG LABTECH Inc., NC), at 37 °C with excitation and emission wavelengths at 494 and 506 nm, respectively.

2.6.7. Statistical analysis

Unless otherwise indicated, all data were expressed as mean ± SEM. Data were statistically analyzed for significant difference; for comparison between two groups, unpaired two-tailed Student's *t*-test were used, while for comparison between more than two groups one-way analysis of variance (ANOVA) followed by Dunnett's post-hoc test were used. A P-value < 0.05 were considered statistically significant.

3. Results

3.1. Sporadic ALS but not C9orf72-ALS astrocytes drives upregulation of P-glycoprotein expression levels in endothelial cells

Using human iPS-derived astrocytes and endothelial cells (ECs) cultured in multi-well plates with trans-well inserts to avoid cell contact and to model *in vitro* the blood-brain barrier, we previously reported that astrocytes derived from both mutant SOD1 and mutant FUS ALS patients increased expression and activity of P-glycoprotein in ECs (Qosa et al., 2016a). Since these ALS-linked mutations represent only a small fraction (~2–3%) of all ALS cases, we wanted to explore whether P-glycoprotein upregulation could also be driven by sporadic and C9orf72-linked ALS astrocytes, which represent the majority of ALS cases (Katyal and Govindarajan, 2017; Su et al., 2014). Surprisingly, C9orf72-ALS astrocytes did not affect P-gp expression in ECs. Instead, sporadic ALS astrocytes upregulated both expression and activity of P-gp (Fig. 1), in accord to what we previously reported for SOD1-A4V astrocytes (Qosa et al., 2016a). Overall, these results are in strong support of the occurrence of a cross-talk between astrocytes and ECs, which ultimately elicits P-gp up-regulation in ECs to alter the blood brain barrier permeability, an effect that is mediated by soluble factors secreted or modulated differently by astrocytes. In line with our *in vitro* findings, analysis of human post-mortem lumber spinal cord tissues revealed upregulation of P-gp expression in samples from sporadic and familial ALS patients, which is consistent with our previous reported work (Jablonski et al., 2012). In contrast, P-gp expression levels were increased in postmortem spinal cord C9orf72 patient tissue sample (Supplementary Fig. 1A).

3.2. Astrocyte-secreted glutamate drives P-glycoprotein upregulation in endothelial cells via NMDA receptor activation

We recently identified an oxidative stress-mediated response mediated by mutant SOD1 astrocytes, which involved Nrf2 activation and NFkB nuclear translocation in ECs as molecular pathways leading to P-gp upregulation (Qosa et al., 2016a). Here, we sought to investigate the nature of the astrocyte-secreted signaling molecule implicated in this upregulation (Malarkey and Parpura, 2008). Multiple lines of published evidence strongly suggested that glutamate is the released factor involved: 1) Glutamate was reported to be released by astrocytes under different pathophysiological conditions to function as gliotransmitter (Harada et al., 2015); 2) Previous studies showed that P-gp expression levels increased after a short exposure of rat brain endothelial microvessels to exogenously applied glutamate (Avemary et al., 2013; Zhu and Liu, 2004); 3) Extracellular brain levels of glutamate are elevated in ALS patients (Heath and Shaw, 2002; Leibowitz et al., 2012). We therefore set out to investigate whether glutamate is the molecule released by ALS astrocytes that ultimately signals to endothelial cells to increase P-gp expression. We previously measured P-gp expression and activity levels in endothelial cells after 48 h of co-culture with astrocytes, a required period of co-cultured time that allows for the maturation of the barrier properties in the *in vitro* trans-well system, such as the establishment of robust TEER values between endothelial cells (Qosa et al., 2016a). We first wanted to confirm whether the primary signaling molecule is indeed a soluble factor secreted by the astrocytes of different genotypes. We exposed the iPS-derived ECs to conditioned medium collected from astrocytes (ACM) of different genotype (ACM collected after 72 h from last medium change) for 30 min, the shortest exposure time reported in the literature to induce upregulation of P-gp in endothelial cells by exogenously applied glutamate (Bauer et al., 2008), washed out the ACM and then assessed P-gp expression levels after additional 6 h to allow sufficient time for *de novo* protein synthesis. As shown in Fig. 2A, P-gp expression was increased by ACM collected from sporadic ALS (ACM-sporadic; +23 ± 4%) and SOD1-A4V astrocytes (ACM-SOD1-A4V; +34 ± 3%), compared to ACM from control subject astrocytes (ACM-CTRL). The upregulation of P-gp expression levels (Fig. 2A) in ECs was comparable to the levels achieved by their co-culturing with iPS-derived astrocytes of the sporadic and mutant SOD1 genotypes (Fig. 1A). Interestingly, C9orf72-ALS astrocytes (ACM-C9orf72) did not affect P-gp expression levels in ECs. To determine if iPS-derived astrocytes from the different ALS genotypes indeed released glutamate, we measured

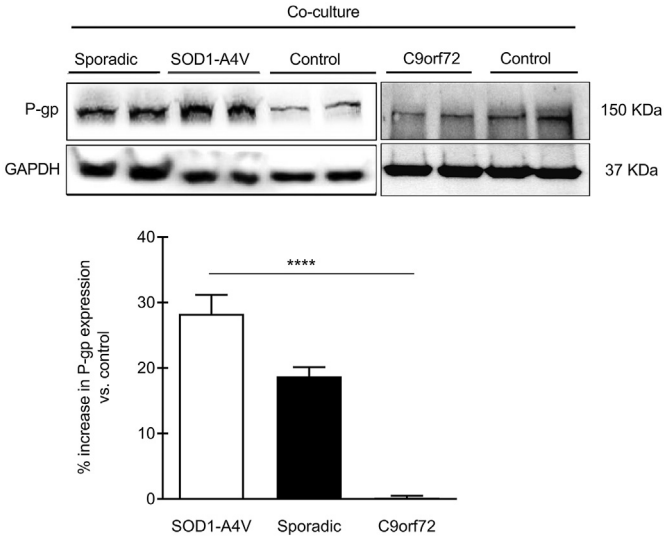

Fig. 1. Expression levels of P-gp in human iPS-derived endothelial cells after co-culture for 24 h with ALS human iPS-derived astrocytes of different genotypes. Co-culturing endothelial cells with either SOD1-A4V, sporadic, but not C9orf72-ALS astrocytes, upregulates P-gp expression. P-gp expression levels were normalized by GAPDH levels in each lane and plotted as % change relative to untreated control, mean ± s.e.m. of three independent experiments. Blots were analyzed for significance using one-way ANOVA, $^{****}P < 0.0001$. Representative western blot showing each experimental group run in duplicate to visualize possible intra-experimental variations. (1-column fitting image.)

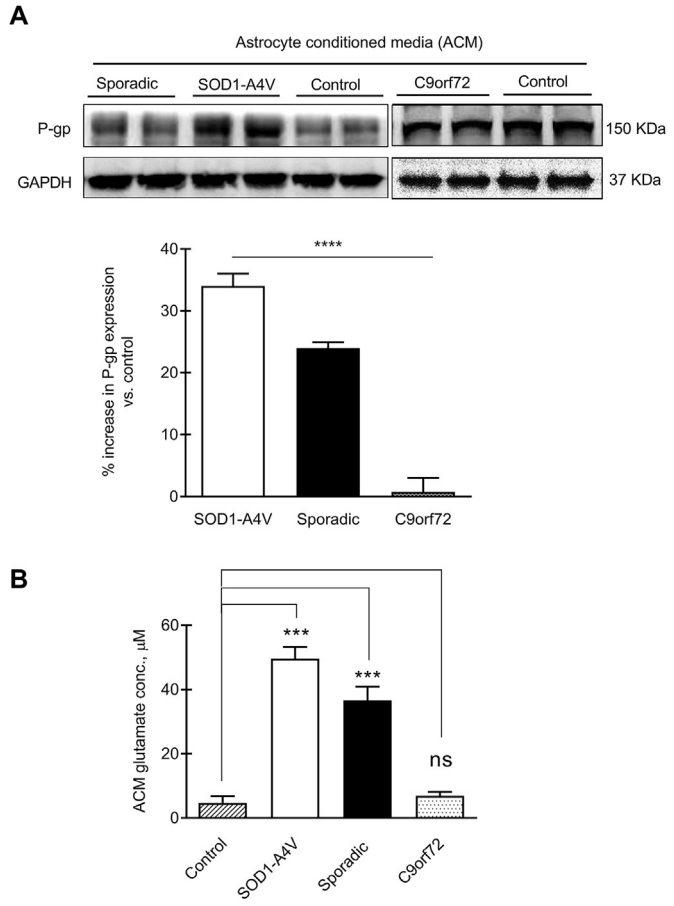

Fig. 2. Expression levels of P-gp in human iPS-derived endothelial cells after incubation with human iPS-derived ALS astrocyte conditioned media (ACM) for 30 min. (A) ACM was collected after 72 h of astrocyte culture, and then human iPS-derived endothelial cells were incubated with ACM for 30 min, followed by removal of ACM and addition of fresh media for 5.5 h. Incubating endothelial cells with ACM from either, SOD1-A4V, sporadic, but not C9orf72-ALS/FTD astrocytes, upregulate its P-gp expression levels compared to control (endothelial cells treated with ACM from non-diseased control subject). Levels of protein expressions were normalized to GAPDH and expressed as variation over control group. Representative western blot showing each experimental group run in duplicate to visualize possible intra-experimental variations. Blots were analyzed for significance using one-way ANOVA, $^{****}P < 0.0001$. (B) Levels of glutamate in ACM collected from ALS-derived astrocytes were measured using Amplex Red Glutamic acid assay kit. Unpaired two-tailed Student's *t*-test was used for statistical significance *vs.* control astrocytes ACM (ns = not significant; *** $P < 0.001$). (1-column fitting image.)

glutamate levels in the ACM using a highly sensitive fluorometric approach (Stobart et al., 2013). ACM-sporadic (36.7 ± 4.1 µM) and ACM-SOD1-A4V (49.6 ± 3.6 µM) have significantly higher levels of glutamate compared to ACM-control (4.6 ± 2.1 µM). Moreover, glutamate levels in ACM-C9orf72 were not statistically different from ACM-control (9.0 ± 1.9 µM; $p = 0.16$).

Next, we examined whether exogenously applied glutamate could increase P-gp expression in human iPS-derived ECs. As shown in Fig. 3A, incubation of human iPS-derived ECs with 100 µM glutamate significantly increased P-gp expression levels compared to untreated control ECs. In addition, pre-treating ECs with the specific NMDA receptor (NMDAR) blocker, MK801 (1 µM), abolished P-gp upregulation mediated by ACM-sporadic and ACM-SOD1-A4V (Fig. 3B, C). These observations suggest that P-gp upregulation is mediated by glutamate *via* NMDARs activation in human iPS-derived ECs, a finding consistent with previous studies reported using rodent EC models (Bauer et al., 2008; Zhu and Liu, 2004), and that glutamate is indeed the gliotransmitter released by human iPS-derived sporadic and SOD1-A4V astrocytes, which drives P-gp upregulation in ECs.

It was previously reported that activation of the NMDAR-COX2 signaling pathway is involved in the glutamate-mediated increase in P-gp expression in the brain microcapillary endothelium (Bauer et al., 2008). We examined whether this pathway was also involved here. We inhibited NMDA receptors with MK801, and in another set of experiments, we inhibited COX2, a downstream enzyme to NMDA receptor-mediated signaling cascade, using celecoxib, a COX2 selective inhibitor (Bauer et al., 2008) and non-steroidal anti-inflammatory drug (NSAID). As shown in Fig. 4, P-gp immunofluorescence signal increased by 4–6 folds when human iPS-derived ECs were incubated with ACM-SOD1-A4V and ACM-sporadic. The extent of P-gp upregulation after ACM treatment as quantified by immunofluorescence signal (Fig. 4) is significantly higher than P-gp upregulation measured by western blot analysis (Fig. 1). This discrepancy could be attributed to differences between antibody/antigen binding affinities due to the denaturing *vs.* non-denaturing conditions between the two assays. When cells were pre-treated with MK801 or celecoxib, both treatments prevented the induction of P-gp upregulation. Similarly to experiments in Fig. 3A, glutamate used as positive control showed consistency in inducing upregulation of P-gp. We noted that in cells that showed P-gp upregulation in response to ACM/or glutamate treatment, P-gp levels decreased below "control level" when treated with MK801 and celecoxib (Fig. 4). This effect was not seen in ECs treated with control ACM. It might be possible that, under our experimental conditions, NMDA receptor and NfkB inhibition works only in cells overstimulated by added/released glutamate.

3.3. Astrocyte conditioned medium increases P-glycoprotein activity

We next looked at whether increased P-gp expression levels were also associated to increased P-gp activity. To examine the effect of ACM-ALS on the function of P-gp we relied on our *in vitro* BBB model, which consisted of human iPS-derived ECs cultured as a monolayer in insert filters placed on top of cell culture wells (Qosa et al., 2016a). Formation of tight junctions between ECs and therefore establishment of barrier properties was examined by measuring trans-endothelial electrical resistance (TEER) and by immunostaining analysis to assess expression of claudine-5, a major constituent protein of tight junctions (TJs) that has a key role in forming and strengthening a barrier between ECs, both *in vitro* and *in vivo* (Luissint et al., 2012). Our *in vitro* BBB model showed consistent expression of claudin-5 (Fig. 5A), and a TEER value of 250 ± 40 Ω/cm^2, confirming formation of intercellular TJs (Wilhelm et al., 2011). In addition, we measured low trans-endothelial permeability of sodium fluorescein (NaF, 2.45 ± 0.35 × 10^{-6} cm/s), further confirming the establishment of barrier function among ECs. In order to examine the activity of P-gp efflux transporter across the EC monolayer, we used Rh123 and LD800, two well-characterized P-gp substrates (Qosa et al., 2016a; Tai et al., 2009) to study vectorial transport of substrates from the basal (B) side, which represents the brain side, to the apical (A) side, which represents blood, and *vice versa* from A to B. The efflux ratio (ER), defined as the ratio of B → A to the A → B apparent permeability (P_{app}) of Rh123 was 4.6 ± 0.56, and for LD800 was 4.5 ± 0.56. A previous study suggested that an ER value of > 2 for a given P-gp substrate is an indication of P-gp efflux transport activity across a given BBB model (Crivori et al., 2006). Furthermore, P-gp activity in our model could be reduced using quinidine (20 µM), a P-gp inhibitor, which decreased ER of Rh123 and LD800 by approximately 50% (Fig. 5B). Collectively, these studies confirmed the functional activity of P-gp in the human iPS endothelial BBB model.

Next, we examined the effect of ACM-ALS on P-gp transport activity. Incubating human iPS-derived ECs with ACM-SOD1-A4V or ACM-sporadic caused significant increase in LD800 transport by 67% and 49%, respectively (Fig. 5C), which indicated an increase in P-gp function.

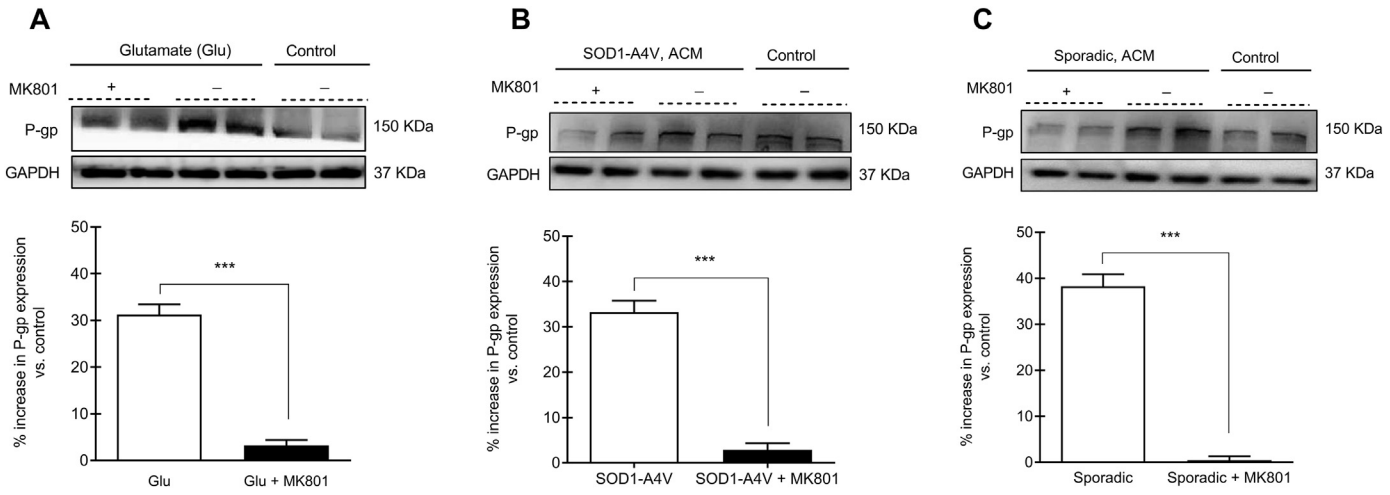

Fig. 3. Glutamate secreted from ALS astrocytes drives P-glycoprotein upregulation in endothelial cells *via* NMDA receptors. Upregulation of P-gp in human iPS-derived endothelial cells after incubation with ALS human iPS-derived astrocyte conditioned media (ACM) for 30 min was abolished by blocking NMDA receptors with 1 μM MK801. Human iPS-derived endothelial cells were pre-incubated with 1 μM MK801 for 15 min, followed by addition of; (A) 100 μM glutamate, as control for P-gp upregulation *via* NMDA receptor stimulation, (B) SOD1-A4V/ACM or (C) Sporadic/ACM for 30 min. Then, media was replaced with fresh media and further incubated for 5.5 h. In each treatment condition, control refers to endothelial cells treated with normal (non-ALS) astrocytes ACM. Levels of protein expressions were measured by western blot, normalized to expression levels of GAPDH and then divided by normalized protein expression of untreated control. Data were plotted as means of percent increase ± s.e.m. of three independent experiments (two-tailed *t*-test, *** $P < 0.001$). (2-column fitting image.)

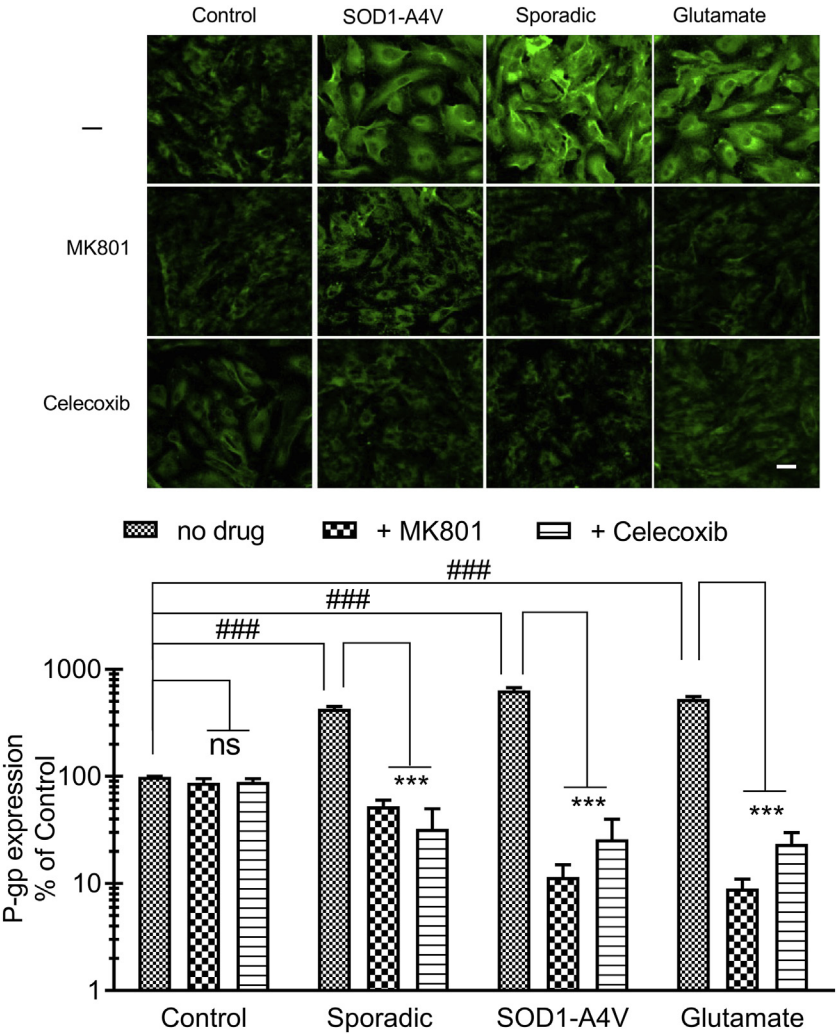

Fig. 4. Glutamate secreted from ALS astrocytes drives P-glycoprotein upregulation in endothelial cells *via* NMDA receptor/COX-2 mediated pathway. Upregulation of P-gp in human iPS-derived endothelial cells after incubation with ALS human iPS-derived astrocyte conditioned media (ACM) for 30 min was abolished by blocking either NMDA receptors with 1 μM MK801 or COX2 with 1 μM celecoxib. Human iPS-derived endothelial cells were pre-incubated with 1 μM MK801 or 1 μM celecoxib, for 15 min, followed by addition of 100 μM glutamate, as positive control for P-gp upregulation *via* NMDA receptor/COX2 stimulation, SOD1-A4V/ACM, Sporadic/ACM, or normal (non-ALS) astrocytes/ACM for 30 min. Media was replaced with fresh media and further incubated for 5.5 h. P-gp expression was assessed by immunofluorescence. P-gp signal was quantified and plotted as mean ± s.e.m. of percent increase over normal (non-ALS) astrocytes/ACM treated controls, (scale bar = μm). Data are average of at least three independent experiments (two-tailed *t*-test; ns = not significant *** or ### $P < 0.001$). (1.5-column fitting image.)

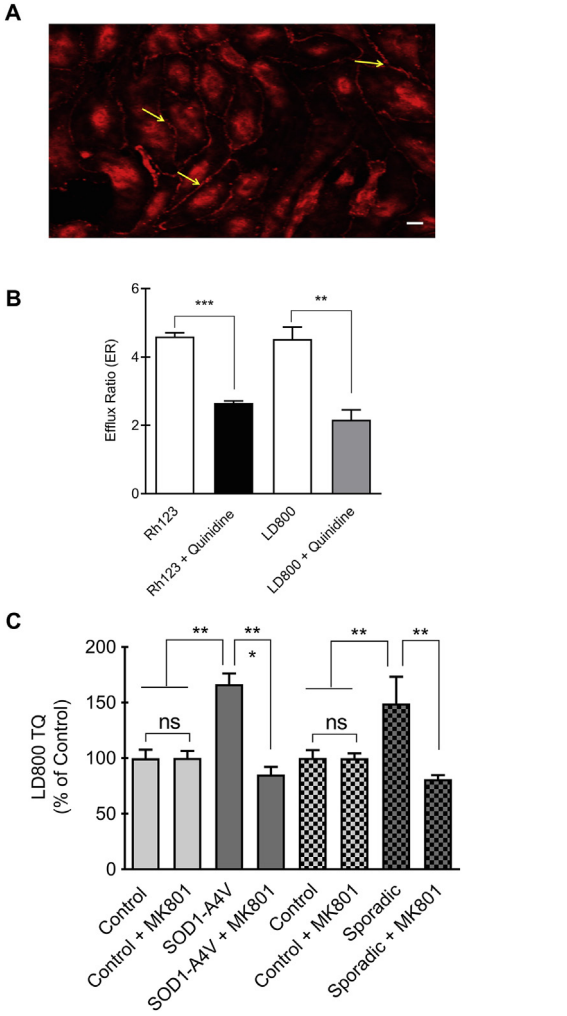

Fig. 5. P-gp activity is enhanced by ACM from human iPS-derived ALS astrocytes. An *in vitro* BBB model was developed by culturing human iPS-derived endothelial cells on transwells. (A) Integrity of modeled human BBB was assessed by measuring expression of claudine-5, a major tight junction protein, by immunocytochemistry, (scale bar = μm). (B) P-gp activity was examined by measuring the efflux ratio (ER), defined as the ratio of B → A to the A → B apparent permeability (P_{app}) of Rh123 and LD800, and by inhibiting P-gp function with 20 μM quinidine. To examine the effect of ALS/ACM on P-gp activity, the human iPS-derived endothelial cells in the *in vitro* BBB model were incubated with ACM from either SOD1-A4V, sporadic, or normal (non-ALS) astrocytes (control), for 30 min, followed by 5.5 h incubation in fresh media alone, then P-gp function was assessed by measuring LD800 permeability as a P-gp probe substrate (C). MK801 (1 μM) was added prior to and during incubation with ACM/ALS. Transport studies data were obtained from at least three independent experiments (two-tailed *t*-test; ns = non significant; ** $P < 0.01$; *** $P < 0.001$). (1-column fitting image.)

To examine whether ACM-ALS enhanced P-gp function through activation of NMDARs, we pre-treated ECs with MK801. As expected, MK801 completely prevented ACM-SOD1-A4V or ACM-sporadic from enhancing endothelial P-gp function (Fig. 5C), indicating that endothelial P-gp upregulation is mediated through astrocyte-secreted glutamate *via* activation of endothelial NMDARs.

We also examined the effect of ACM-SOD1-A4V and ACM-sporadic on P-gp function on *ex-vivo* isolated brain capillaries from wild type rats. Brain capillaries can be isolated and remain viable for up to 12 h, maintaining expression and function of drug efflux transporters such as P-gp, and proving a more physiological system in which to test P-gp regulatory pathways (Hartz et al., 2010). Zhu and Liu reported that glutamate enhances the functional activity of P-gp in rat brain capillary endothelium *ex-vivo*, an effect blocked by MK801 (Zhu and Liu, 2004). P-gp is localized to the capillary lumen, and thus, addition of P-gp fluorescent substrate, NBD-cyclosporin A, is expected to accumulate as green fluorescence inside the capillaries. An increase in the transport activity of P-gp correlates with enhanced fluorescent intensity of accumulated NDB-CSA. As shown in Fig. 6, exposure of isolated brain capillaries to patient-derived SOD1-A4V and sporadic astrocyte-conditioned media significantly enhanced NBD-CSA luminal accumulation by approximately 6-fold, compared to control treated capillaries. The increase in luminal fluorescence was completely inhibited by both MK801 and celecoxib (Fig. 6). Exogenous application of glutamate was again used as control to increase P-gp function and showed consistent results.

3.4. Astrocyte conditioned media increase intracellular free-calcium levels in endothelial cells

Activation of NMDA receptors in ECs of the BBB leads to increased intracellular free calcium levels (Neuhaus et al., 2011). We examined whether exposure to ACM would increase intracellular free calcium levels in ECs. Human iPS-derived ECs preloaded with the Ca^{2+} indicator Fluo-4 AM were exposed to ACM-SOD1-A4V or ACM/sporadic. As shown in Fig. 7A–C, this increased the fluorescence of Fluo-4 AM in ECs by approximately 120% in a rapid and persistent manner over 45 min of incubation period. The area under the curve (AUC) of the Flou-4 AM fluorescence over time (Fig. 7E) increased by 2.0 fold (from 1004 to 2057) and 2.1 fold (AUC increased from 1004 to 2068) after incubating iPS endothelial cells with either ACM-SOD1-A4V or ACM-sporadic, respectively. Glutamate, 100 μM, which was used for comparison, increased intracellular free Ca^{2+}-mediated fluorescence by 1.8 fold (AUC from 1004 to 1795) in ECs compared to vehicle-treated control group (Fig. 7D). To determine whether changes in free Ca^{2+} were due to astrocyte-secreted glutamate and activation of NMDARs, human iPS-derived ECs were treated with MK-801, which inhibited the increase in free Ca^{2+} levels mediated by ACM/SOD1-A4V, ACM/sporadic or 100 μM glutamate throughout the 45 min of incubation time by approximately 72%, 64%, and 58% (Fig. 7A–D). AUCs were also decreased by 69%, 63% and 62% (Fig. 7E). These findings indicated that the increase in intracellular calcium was largely mediated by glutamate-secreted astrocytes through activation of the NMDAR complex.

3.5. Activation of NFκB is downstream the NMDAR-mediated upregulation of P-gp in endothelial cells

Previous lines of evidence showed that a translocation of NFκB to the nucleus of endothelial cells is preceding P-gp upregulation (Bauer et al., 2008; Qosa et al., 2016a). In addition, activation of NMDARs in the ECs of the BBB triggers P-gp upregulation (Bauer et al., 2008). Therefore, we examined whether P-gp upregulation mediated by ACM-ALS activation of NMDARs and COX-II signaling would also involve NFκB nuclear translocation. Robust NFκB nuclear translocation occurred in human iPS-derived ECs upon exposure to 100 μM glutamate, ACM-SOD1-A4V, or ACM-sporadic, compared to cells exposed to ACM-CTRL (Fig. 8). Furthermore, the activity of NFκB was abolished when ECs were pretreated with MK-801 or celecoxib, suggesting that stimulation of NFκB was mediated through NMDA receptor signaling pathway.

4. Discussion

Several pre-clinical and clinical studies reported elevated glutamate levels both in brain extracellular fluids (ECF) and plasma of ALS patients and animal models (Andreadou et al., 2008; Spreux-Varoquaux et al., 2002). Glutamate ECF levels are essentially controlled by glutamate transporters and by the homeostatic balance of the glutamate-glutamine cycle occurring in astrocytes and neurons (Danbolt, 2001;

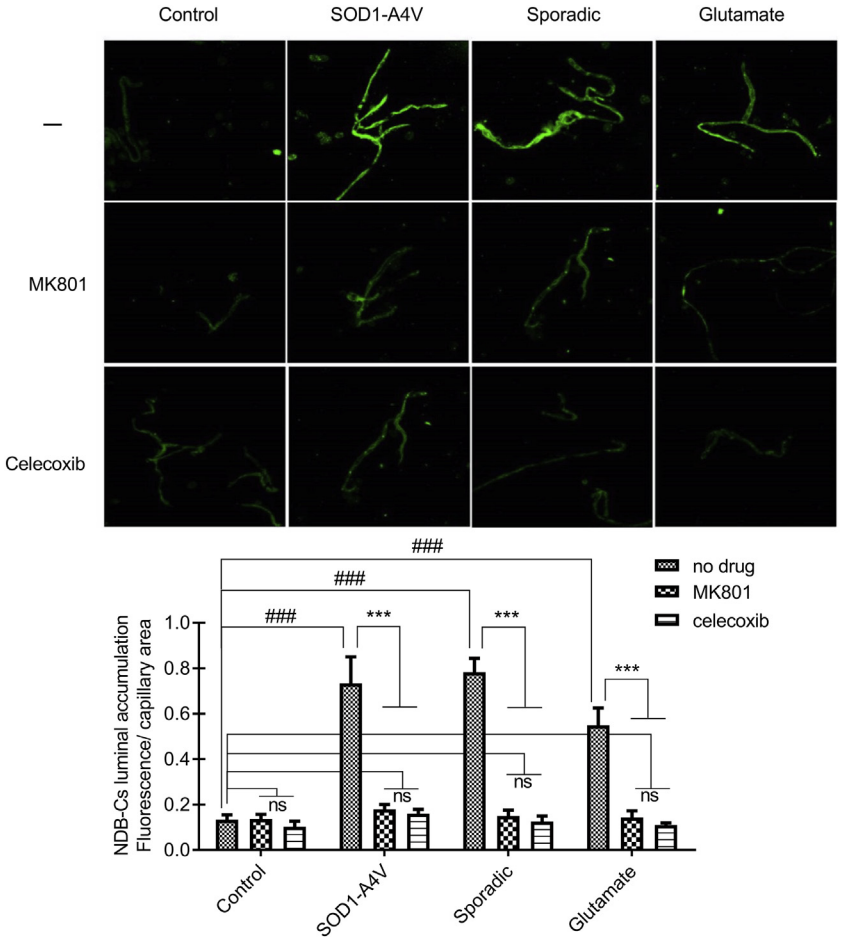

Fig. 6. ALS-derived ACM enhances P-glycoprotein activity in isolated brain capillaries *via* NMDA receptor/COX2 mediated pathway. Increase in P-gp activity in isolated, viable rat brain capillaries after incubation with ALS human iPS-derived astrocyte conditioned media (ACM) was abolished by either blocking NMDA receptors with 1 μM MK801 or COX2 with 1 μM celecoxib. Human iPS endothelial cells were pre-incubated with 1 μM MK801 or 1 μM celecoxib, for 15 min, followed by addition of 100 μM glutamate, SOD1-A4V/ACM, or sporadic/ACM for 30 min. Then, the medium was removed and completely replaced with fresh one, cells were further incubated for 5.5 h and NBD-CSA luminal accumulation was assessed by confocal microscopy. Luminal green fluorescence of NBD-CSA accumulation was measured and plotted as arbitrary unit of at least three independent experiments (two-tailed *t*-test; ns = not significant; *** or ### $P < 0.001$). (1.5-column fitting image.)

Harada et al., 2015). In addition, the plasma acts as a sink for glutamate in the central nervous system, from which is extruded across the BBB (Helms et al., 2012; Teichberg et al., 2009). A prolonged unbalance of this glutamate homeostasis leads to excitotoxicity, which contributes to the neurodegeneration and neuronal death seen in diseases such as ALS and epilepsy (Harada et al., 2015; Tian et al., 2005). Aberrantly elevated glutamate levels in the ECF could also lead to upregulation of P-gp in endothelial cells at the BBB, *via* activation of NMDA receptors expressed by endothelial cells (Potschka, 2010) (Avemary et al., 2013; Bauer et al., 2008). While P-gp upregulation at the BBB could provide a protective mechanism to guard the vulnerable brain from blood-born toxins or potentially toxic catabolites, it is however considered a major hurdle against the passage of therapeutic agents to the CNS, the so called "P-gp-mediated pharmacoresistance" (Mohamed et al., 2017). Evidence for a glutamate-induced pharmacoresistance has been provided in epilepsy; however, whether the same signaling pathway brings about pharmacoresistance in ALS is not known. The aim of our study was to understand whether glutamate and P-gp upregulation at the BBB are linked in ALS. Our previous findings on a possible involvement of astrocyte-released soluble factors in regulating the function and expression of P-gp in endothelial cells at the BBB in ALS, as well as the proven astrocytes role in glutamate uptake and release, led us to study whether glutamate could have been the released soluble factor mediating the upregulation of P-gp at the BBB (Qosa et al., 2016a). P-gp activity in the mutant SOD1-G93A animal model of ALS dictates the overall BBB permeability of P-gp substrates (Jablonski et al., 2012; Qosa et al., 2016a). In addition, we reported that astrocytes derived from ALS patients cause P-gp upregulation through various mechanisms that converge into nuclear translocation of NFκB (Qosa et al., 2016a). In the current study, we found that exposure of human iPS endothelial cells to conditioned media collected from SOD1-A4V or sporadic human iPS-derived astrocytes, but not C9orf72 astrocytes, increased expression and activity of P-gp *via* NMDA receptor activation, an effect that is mimicked by exogenous application of glutamate. In normal physiologic conditions, glutamate levels in brain ECF are maintained between 1 and 10 μM; however, in CNS areas affected by ALS the glutamate levels were reported to be considerably higher (Castillo et al., 2016; Foran and Trotti, 2009). Previous studies reported that glutamate levels in epilepsy were between 10 and 100 μM, which were suggested to induce P-gp upregulation (Bauer et al., 2008; Ronne-Engstrom et al., 1992; Ueda and Tsuru, 1995). Measurements of glutamate concentration *in vitro* in SOD1-A4V or sporadic astrocyte conditioned media showed approximately 10-fold higher glutamate levels compared to control (Fig. 2B). In addition, elevated glutamate levels correlated well with the P-gp upregulation in endothelial cells. The association between glutamate and P-gp expression levels was also strengthened by the evidence of lack of effect by C9orf72 astrocyte conditioned medium, in which glutamate concentration is not significantly different from control. We previously reported a robust upregulation of P-gp in post-mortem spinal cord tissues of SOD1-A4V and sporadic ALS patients (Jablonski et al., 2012), and here we showed that this upregulation also occurred in the spinal cord of a C9orf72-ALS patient. The discrepancy with *in vitro* data could be explained by the existence of specific mechanisms of regulation that are occurring *in vivo* and that may not engage astrocytes, or glutamate in particular, and might involve instead different signaling cascades and the contribution of other cell types, which are absent in our *in vitro* BBB model (*i.e.* pericytes). Future studies are needed to study the mechanisms of P-gp regulation at the BBB in C9orf72-ALS.

Earlier reports revealed that P-gp is upregulated upon exposure of

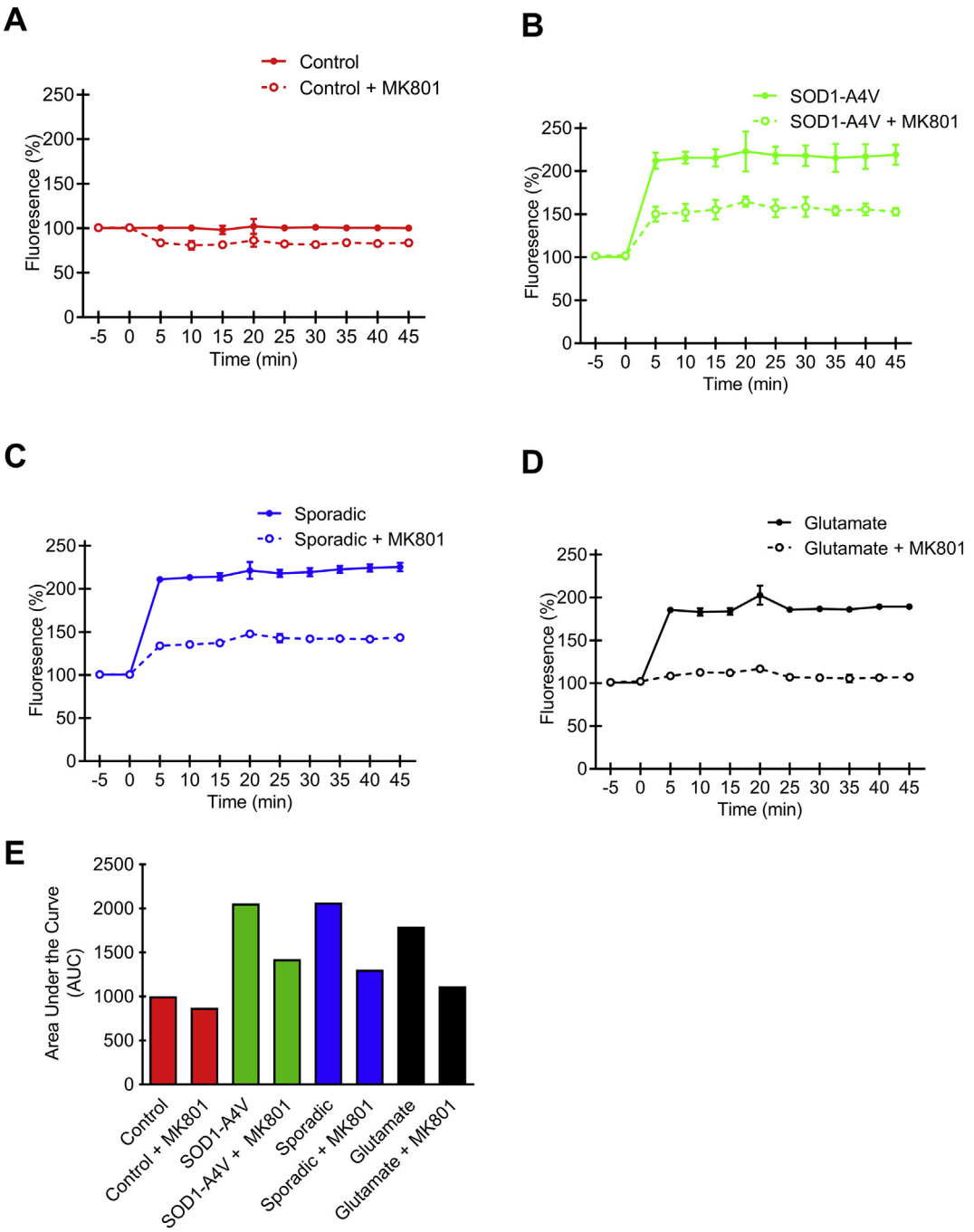

Fig. 7. ALS-derived ACM increase intracellular Ca^{2+} levels in human iPS-derived endothelial cells mainly *via* NMDA receptor mediated pathway. Intracellular free calcium levels under different conditions of treatment with ALS-derived ACM from normal (non-ALS) astrocytes (Control) (A), SOD1-A4V (B), sporadic (C), and glutamate (D), were determined by assessing the change in fluorescence intensity in Fluo-4-loaded cells. Human iPS-derived endothelial cells were loaded 2.5 μM Fluo-4 AM, then calcium levels were measured by determining baseline fluorescence in cells loaded with Fluo-4 AM alone for 5 min, followed by addition of ACM alone or with the NMDA receptor antagonist, 1 μM MK-801. Measurement of fluorescence signal continued for 45 min at 37 °C with excitation and emission wavelengths at 494 and 506 nm, respectively. Area under the curve (AUC) of the calcium fluorescence profiles was plotted as bar-chart for comparison between different ACM-derived ALS treatments (E). Experiments were performed in 96 well plates for two independent experiments with six replicates for each ACM treatment group. (1.5-column fitting image.)

isolated brain capillaries to glutamate (Bauer et al., 2008; Zhu and Liu, 2004), possibly through a pathway that involves activation of NMDA receptors, increase in intracellular free calcium levels, phospholipase A2-mediated arachidonic acid release and production of prostaglandin E2 by cyclooxygenase-2 (van Vliet et al., 2010; Zibell et al., 2009). In agreement, we found that blocking NMDA receptors and COX2, with either MK801 or celecoxib, significantly reduced the effect of mutant SOD1 and sporadic astrocytes conditioned media on P-gp expression and intracellular free calcium levels in endothelial cells. Interestingly, the catalytic activity of COX2 is dramatically increased in the spinal cord of the mutant SOD1 mouse model of ALS as well as in postmortem spinal cord samples of sporadic ALS patients (Almer et al., 2001), an evidence which supports the notion of glutamate-mediated P-gp upregulation in the mutant SOD1 and sporadic form of ALS. Therapeutic targeting COX2 with inhibitors was suggested for treatment of diseases that are associated with inflammation, such as arthritis, multiple

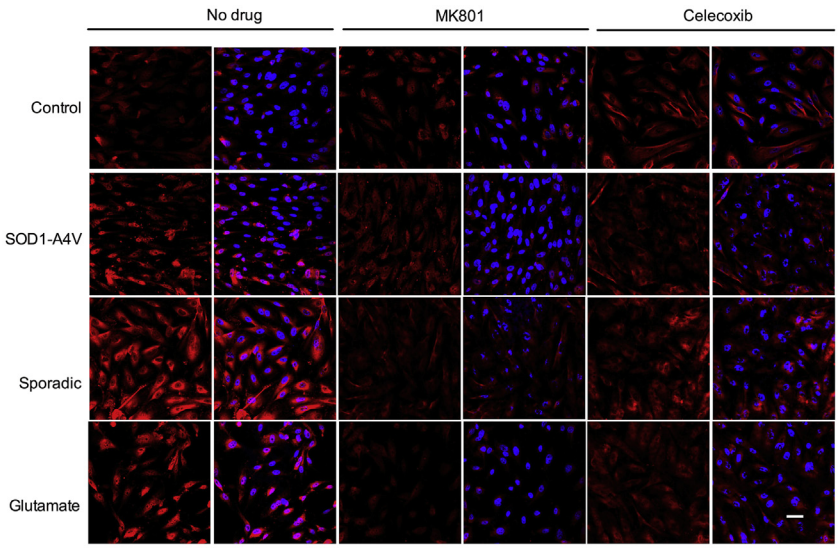

Fig. 8. ALS-derived ACM stimulates NFκB nuclear translocation in human iPS endothelial cells *via* NMDA receptor/ COX-2 mediated pathway. Nuclear translocation of NFκB in iPS human endothelial cells after incubation with ALS human iPS-derived astrocyte conditioned media (ACM) was abolished by blocking either NMDA receptors with 1 μM MK801 or COX-2 with 1 μM celecoxib. Human iPS endothelial cells were pre-incubated with 1 μM MK-801 or 1 μM celecoxib, for 15 min, followed by 30 min incubation with normal (non-ALS) astrocytes (Control)/ACM, SOD1-A4V/ACM, sporadic/ACM, or 100 μM glutamate, as a positive control for NFκB stimulation *via* NMDA receptor/COX2 stimulation. Then, media was removed and completely replaced with fresh media and incubated for 5.5 h. After that levels of protein expressions were measured by immunocytochemical analysis of at least three independent experiments. Blue color represents DAPI (4′,6-diamidino-2-phenylindole) staining of Nuclei, and red color represents Alexa Fluor 546 secondary antibody staining of NFκB. (2-column fitting image).

sclerosis, Alzheimer's disease and ALS (Maihofner et al., 2003; Turini and DuBois, 2002). Indeed, COX2 inhibition has shown promise in overcoming glutamate-mediated P-gp upregulation in epilepsy, as well as in Parkinson's animal models. Obstructing glutamate signaling cascade by selective inhibition of COX2 with celecoxib counteracted P-gp upregulation by glutamate and improved brain penetration of the antiepileptic drug phenobarbital in a chronic model of drug-resistant temporal lobe epilepsy in rats (Schlichtiger et al., 2010). Similarly, celecoxib was shown to inhibit COX2 in isolated rat capillaries and was accompanied by a decrease in P-gp activity (Bauer et al., 2008). Therefore, targeting COX-2 by inhibitors could be a useful strategy to overcome P-gp-mediated pharmacoresistance in ALS as well.

In addition to its established role in neuroinflammation, previous studies suggested an involvement of NFκB in P-gp expression levels regulation at the BBB (Bauer et al., 2008; Deng et al., 2001; Qosa et al., 2015). NF-κB is activated in astrocytes in familial and sporadic ALS patients as well as in the SOD1-G93A mouse model over disease progression (Frakes et al., 2014a; Swarup et al., 2011). We showed that NFκB nuclear translocation in endothelial cells is dependent on NMDA receptor and COX2 activation. Astrocytes derived from mutant SOD1 patients drive endothelial cells to increase production of reactive oxygen species (ROS) and to activate Nrf2 pathway, which stimulates NFκB-mediated P-gp upregulation (Qosa et al., 2016a). NMDA receptor activation by glutamate have been previously linked to increased ROS production in rat brain microvessel endothelial cells (Zhu and Liu, 2004). It is therefore possible that NFκB activation and the subsequent upregulation of P-gp expression in endothelial cells in ALS could be ultimately triggered by one priming event that is the activation of NMDA receptors by glutamate. All these pathways could then eventually converge in NFκB nuclear translocation and increased MDR1 gene transcription and translation. This makes targeting NFκB another attractive therapeutic strategy to control P-gp expression in ALS. However, since NFκB has a key role in regulating several cellular processes in different cell types in the body, it is important to specifically target NFκB at the capillary endothelium of the BBB to avoid potential off-target associated toxicity. Interestingly, few studies have reported selective inhibition of endothelial NFκB in inflammatory diseases such as arthritis and atherosclerosis (Gareus et al., 2008; Sehnert et al., 2015). For example, specific inhibition of NFκB at the arterial wall endothelium was achieved by ablation of NEMO/*Ik*Kγ or expression of dominant-negative *Ik*Bα specifically in endothelial cells, which resulted in strongly reduced atherosclerotic plaque formation in atherosclerotic mice model (Gareus et al., 2008). More recently, Sehnert and colleagues developed an *E*-selectin–specific NF-κB inhibitor, known as “sneaking ligand construct” (SLC), which is a fusion protein that selectively target activated endothelial cells (Sehnert et al., 2013). This cell type-specific NF-κB inhibition could provide a useful approach to target cells that actively express NF-κB, such as those at the capillary endothelium of the BBB in ALS.

Collectively, our findings are pointing at glutamate as the soluble factor released by SOD1-A4V and sporadic ALS astrocytes that mediate P-gp upregulation at the BBB endothelium. Studies on mutant SOD1 pre-clinical model of ALS showed that P-gp upregulation is occurring beginning at disease onset, a phase of disease that correlates with elevated glutamate concentrations in the CSF (Spreux-Varoquaux et al., 2002). Previous findings suggest that these high glutamate concentrations could reflect the intensity of cellular damage in the spinal cord (Spreux-Varoquaux et al., 2002). Here, we speculate that high glutamate levels in brain and spinal cord of ALS patients could trigger P-gp upregulation. While high glutamate levels observed in our study in ALS patients astrocytes could be attributed to altered glutamate release, multiple other mechanisms are also reported in ALS to increase brain interstitial fluid glutamate levels, such as defective high affinity glutamate transport by astrocytes and neurons, impairment in the cystine/glutamate exchanger, reversal and/or impairment of glutamate transporters activity (Foran and Trotti, 2009; Qosa et al., 2016b; Rothstein et al., 1992). In addition to astrocytes and neurons, the BBB has an important role in maintaining low ECF glutamate levels by expelling glutamate from the brain utilizing EAAT transporters expressed by capillary endothelium (Hawkins, 2009). Interestingly, Liu and colleagues suggested that P-gp has a role in regulating glutamate transport across the BBB (Liu and Liu, 2001). This finding may argue that P-gp upregulation in ALS is a feedback mechanism to enhance the removal of abnormally high glutamate ECF levels in an attempt to attenuate neurototoxicity. Nonetheless, this feedback mechanism may constitute a hurdle for CNS-targeted therapeutics to reach their site of action. We have previously shown that P-gp overexpression at the BBB is a major barrier for riluzole to cross the BBB and reach its therapeutic targets (Jablonski et al., 2012 #7). Therefore, the outcome of P-gp inhibition showed be carefully assessed so that the benefits outweigh possible adverse effects. Future studies may further examine the glutamate-mediated P-gp upregulation hypothesis in animal models of ALS and examine whether inhibiting NMDAR, COX2 or NF-κB would counteract P-gp function and improve brain penetration of ALS therapeutics.

Supplementary data to this article can be found online at https://doi.org/10.1016/j.expneurol.2019.04.002.

Funding

This work was supported by the National Institutes of Health [grant number RO1-NS074886 to DT) and by Target ALS (to DT and PP).

Declaration of interest

None.

References

Abbott, N.J., 2013. Blood-brain barrier structure and function and the challenges for CNS drug delivery. J. Inherit. Metab. Dis. 36, 437–449.
Abbott, N.J., Friedman, A., 2012. Overview and introduction: the blood-brain barrier in health and disease. Epilepsia 53 (Suppl. 6), 1–6.
Abbott, N.J., Patabendige, A.A., Dolman, D.E., Yusof, S.R., Begley, D.J., 2010. Structure and function of the blood-brain barrier. Neurobiol. Dis. 37, 13–25.
Almer, G., Guegan, C., Teismann, P., Naini, A., Rosoklija, G., Hays, A.P., Chen, C., Przedborski, S., 2001. Increased expression of the pro-inflammatory enzyme cyclooxygenase-2 in amyotrophic lateral sclerosis. Ann. Neurol. 49, 176–185.
Andreadou, E., Kapaki, E., Kokotis, P., Paraskevas, G.P., Katsaros, N., Libitaki, G., Petropoulou, O., Zis, V., Sfagos, C., Vassilopoulos, D., 2008. Plasma glutamate and glycine levels in patients with amyotrophic lateral sclerosis. In Vivo 22, 137–141.
Avemary, J., Salvamoser, J.D., Peraud, A., Remi, J., Noachtar, S., Fricker, G., Potschka, H., 2013. Dynamic regulation of P-glycoprotein in human brain capillaries. Mol. Pharm. 10, 3333–3341.
Baello, S., Iqbal, M., Gibb, W., Matthews, S.G., 2016. Astrocyte-mediated regulation of multidrug resistance p-glycoprotein in fetal and neonatal brain endothelial cells: age-dependent effects. Phys. Rep. 4.
Bauer, B., Hartz, A.M., Pekcec, A., Toellner, K., Miller, D.S., Potschka, H., 2008. Seizure-induced up-regulation of P-glycoprotein at the blood-brain barrier through glutamate and cyclooxygenase-2 signaling. Mol. Pharmacol. 73, 1444–1453.
Boulting, G.L., Kiskinis, E., Croft, G.F., Amoroso, M.W., Oakley, D.H., Wainger, B.J., Williams, D.J., Kahler, D.J., Yamaki, M., Davidow, L., Rodolfa, C.T., Dimos, J.T., Mikkilineni, S., MacDermott, A.B., Woolf, C.J., Henderson, C.E., Wichterle, H., Eggan, K., 2011. A functionally characterized test set of human induced pluripotent stem cells. Nat. Biotechnol. 29, 279–286.
Castillo, J., Loza, M.I., Mirelman, D., Brea, J., Blanco, M., Sobrino, T., Campos, F., 2016. A novel mechanism of neuroprotection: blood glutamate grabber. J. Cereb. Blood Flow Metab. 36, 292–301.
Crivori, P., Reinach, B., Pezzetta, D., Poggesi, I., 2006. Computational models for identifying potential P-glycoprotein substrates and inhibitors. Mol. Pharm. 3, 33–44.
Danbolt, N.C., 2001. Glutamate uptake. Prog. Neurobiol. 65, 1–105.
Deng, L., Lin-Lee, Y.C., Claret, F.X., Kuo, M.T., 2001. 2-acetylaminofluorene up-regulates rat mdr1b expression through generating reactive oxygen species that activate NF-kappa B pathway. J. Biol. Chem. 276, 413–420.
Felix, R.A., Barrand, M.A., 2002. P-glycoprotein expression in rat brain endothelial cells: evidence for regulation by transient oxidative stress. J. Neurochem. 80, 64–72.
Foran, E., Trotti, D., 2009. Glutamate transporters and the excitotoxic path to motor neuron degeneration in amyotrophic lateral sclerosis. Antioxid. Redox Signal. 11, 1587–1602.
Frakes, A.E., Ferraiuolo, L., Haidet-Phillips, A.M., Schmelzer, L., Braun, L., Miranda, C.J., Ladner, K.J., Bevan, A.K., Foust, K.D., Godbout, J.P., Popovich, P.G., Guttridge, D.C., Kaspar, B.K., 2014a. Microglia induce motor neuron death via the classical NF-kappaB pathway in amyotrophic lateral sclerosis. Neuron 81, 1009–1023.
Frakes, Ashley E., Ferraiuolo, L., Haidet-Phillips, Amanda M., Schmelzer, L., Braun, L., Miranda, Carlos J., Ladner, Katherine J., Bevan, Adam K., Foust, Kevin D., Godbout, Jonathan P., Popovich, Phillip G., Guttridge, Denis C., Kaspar, Brian K., 2014b. Microglia induce motor neuron death via the classical NF-κB pathway in amyotrophic lateral sclerosis. Neuron 81, 1009–1023.
Gareus, R., Kotsaki, E., Xanthoulea, S., van der Made, I., Gijbels, M.J., Kardakaris, R., Polykratis, A., Kollias, G., de Winther, M.P., Pasparakis, M., 2008. Endothelial cell-specific NF-kappaB inhibition protects mice from atherosclerosis. Cell Metab. 8, 372–383.
Haidet-Phillips, A.M., Roybon, L., Gross, S.K., Tuteja, A., Donnelly, C.J., Richard, J.P., Ko, M., Sherman, A., Eggan, K., Henderson, C.E., Maragakis, N.J., 2014. Gene profiling of human induced pluripotent stem cell-derived astrocyte progenitors following spinal cord engraftment. Stem Cells Transl. Med. 3, 575–585.
Harada, K., Kamiya, T., Tsuboi, T., 2015. Gliotransmitter release from astrocytes: functional, developmental, and pathological implications in the brain. Front. Neurosci. 9, 499.
Hardiman, O., Al-Chalabi, A., Chio, A., Corr, E.M., Logroscino, G., Robberecht, W., Shaw, P.J., Simmons, Z., van den Berg, L.H., 2017. Amyotrophic lateral sclerosis. Nat. Rev. Dis. Prim. 3, 17071.
Hartz, A.M., Bauer, B., Fricker, G., Miller, D.S., 2004. Rapid regulation of P-glycoprotein at the blood-brain barrier by endothelin-1. Mol. Pharmacol. 66, 387–394.
Hartz, A.M., Miller, D.S., Bauer, B., 2010. Restoring blood-brain barrier P-glycoprotein reduces brain amyloid-beta in a mouse model of Alzheimer's disease. Mol. Pharmacol. 77, 715–723.
Hawkins, R.A., 2009. The blood-brain barrier and glutamate. Am. J. Clin. Nutr. 90, 867S–874S.
Heath, P.R., Shaw, P.J., 2002. Update on the glutamatergic neurotransmitter system and the role of excitotoxicity in amyotrophic lateral sclerosis. Muscle Nerve 26, 438–458.
Helms, H.C., Madelung, R., Waagepetersen, H.S., Nielsen, C.U., Brodin, B., 2012. In vitro evidence for the brain glutamate efflux hypothesis: brain endothelial cells cocultured with astrocytes display a polarized brain-to-blood transport of glutamate. Glia 60, 882–893.
Jablonski, M.R., Jacob, D.A., Campos, C., Miller, D.S., Maragakis, N.J., Pasinelli, P., Trotti, D., 2012. Selective increase of two ABC drug efflux transporters at the blood-spinal cord barrier suggests induced pharmacoresistance in ALS. Neurobiol. Dis. 47, 194–200.
Johnson, A.J., Hsu, A.L., Lin, H.P., Song, X., Chen, C.S., 2002. The cyclo-oxygenase-2 inhibitor celecoxib perturbs intracellular calcium by inhibiting endoplasmic reticulum Ca2+-ATPases: a plausible link with its anti-tumour effect and cardiovascular risks. Biochem. J. 366, 831–837.
Katyal, N., Govindarajan, R., 2017. Shortcomings in the current amyotrophic lateral sclerosis trials and potential solutions for improvement. Front. Neurol. 8, 521.
Leibowitz, A., Boyko, M., Shapira, Y., Zlotnik, A., 2012. Blood glutamate scavenging: insight into neuroprotection. Int. J. Mol. Sci. 13, 10041–10066.
Lippmann, Ethan S., Al-Ahmad, Abraham, Azarin, Samira M., Palecek, Sean P., Shusta, Eric V., 2014. A retinoic acid-enhanced, multicellular human blood-brain barrier model derived from stem cell sources. Sci. Rep. 4, 4160 (PMID: 24561821).
Liu, X.D., Liu, G.Q., 2001. P glycoprotein regulated transport of glutamate at blood brain barrier. Acta Pharmacol. Sin. 22, 111–116.
Loscher, W., Luna-Tortos, C., Romermann, K., Fedrowitz, M., 2011. Do ATP-binding cassette transporters cause pharmacoresistance in epilepsy? Problems and approaches in determining which antiepileptic drugs are affected. Curr. Pharm. Des. 17, 2808–2828.
Luissint, A.C., Artus, C., Glacial, F., Ganeshamoorthy, K., Couraud, P.O., 2012. Tight junctions at the blood brain barrier: physiological architecture and disease-associated dysregulation. Fluids Barriers CNS 9, 23.
Maihofner, C., Probst-Cousin, S., Bergmann, M., Neuhuber, W., Neundorfer, B., Heuss, D., 2003. Expression and localization of cyclooxygenase-1 and -2 in human sporadic amyotrophic lateral sclerosis. Eur. J. Neurosci. 18, 1527–1534.
Malarkey, E.B., Parpura, V., 2008. Mechanisms of glutamate release from astrocytes. Neurochem. Int. 52, 142–154.
Miller, D.S., Bauer, B., Hartz, A.M., 2008. Modulation of P-glycoprotein at the blood-brain barrier: opportunities to improve central nervous system pharmacotherapy. Pharmacol. Rev. 60, 196–209.
Mohamed, L.A., Keller, J.N., Kaddoumi, A., 2016. Role of P-glycoprotein in mediating rivastigmine effect on amyloid-beta brain load and related pathology in Alzheimer's disease mouse model. Biochim. Biophys. Acta 1862, 778–787.
Mohamed, L.A., Markandaiah, S., Bonanno, S., Pasinelli, P., Trotti, D., 2017. Blood-brain barrier driven pharmacoresistance in amyotrophic lateral sclerosis and challenges for effective drug therapies. AAPS J. 19, 1600–1614.
Neuhaus, W., Freidl, M., Szkokan, P., Berger, M., Wirth, M., Winkler, J., Gabor, F., Pifl, C., Noe, C.R., 2011. Effects of NMDA receptor modulators on a blood-brain barrier in vitro model. Brain Res. 1394, 49–61.
Noursadeghi, M., Tsang, J., Haustein, T., Miller, R.F., Chain, B.M., Katz, D.R., 2008. Quantitative imaging assay for NF-kappaB nuclear translocation in primary human macrophages. J. Immunol. Methods 329, 194–200.
Potschka, H., 2010. Targeting regulation of ABC efflux transporters in brain diseases: a novel therapeutic approach. Pharmacol. Ther. 125, 118–127.
Qosa, H., Miller, D.S., Pasinelli, P., Trotti, D., 2015. Regulation of ABC efflux transporters at blood-brain barrier in health and neurological disorders. Brain Res. 1628, 298–316.
Qosa, H., Lichter, J., Sarlo, M., Markandaiah, S.S., McAvoy, K., Richard, J.P., Jablonski, M.R., Maragakis, N.J., Pasinelli, P., Trotti, D., 2016a. Astrocytes drive upregulation of the multidrug resistance transporter ABCB1 (P-Glycoprotein) in endothelial cells of the blood-brain barrier in mutant superoxide dismutase 1-linked amyotrophic lateral sclerosis. Glia 64, 1298–1313.
Qosa, H., Mohamed, L.A., Alqahtani, S., Abuasal, B.S., Hill, R.A., Kaddoumi, A., 2016b. Transporters as drug targets in neurological diseases. Clin. Pharmacol. Ther. 100, 441–453.
Ronne-Engstrom, E., Hillered, L., Flink, R., Spannare, B., Ungerstedt, U., Carlson, H., 1992. Intracerebral microdialysis of extracellular amino acids in the human epileptic focus. J. Cereb. Blood Flow Metab. 12, 873–876.
Rosenblum, L.T., Trotti, D., 2017. EAAT2 and the molecular signature of amyotrophic lateral sclerosis. Adv. Neurobiol. 16, 117–136.
Rothstein, J.D., Martin, L.J., Kuncl, R.W., 1992. Decreased glutamate transport by the brain and spinal cord in amyotrophic lateral sclerosis. N. Engl. J. Med. 326, 1464–1468.
Schlichtiger, J., Pekcec, A., Bartmann, H., Winter, P., Fuest, C., Soerensen, J., Potschka, H., 2010. Celecoxib treatment restores pharmacosensitivity in a rat model of pharmacoresistant epilepsy. Br. J. Pharmacol. 160, 1062–1071.
Sehnert, B., Burkhardt, H., Wessels, J.T., Schroder, A., May, M.J., Vestweber, D., Zwerina, J., Warnatz, K., Nimmerjahn, F., Schett, G., Dubel, S., Voll, R.E., 2013. NF-kappaB inhibitor targeted to activated endothelium demonstrates a critical role of endothelial NF-kappaB in immune-mediated diseases. Proc. Natl. Acad. Sci. U. S. A. 110, 16556–16561.
Sehnert, B., Burkhardt, H., May, M.J., Zwerina, J., Voll, R.E., 2015. Sneaking-ligand fusion proteins attenuate serum transfer arthritis by endothelium-targeted NF-kappaB inhibition. Methods Mol. Biol. 1280, 579–591.
Spreux-Varoquaux, O., Bensimon, G., Lacomblez, L., Salachas, F., Pradat, P.F., Le Forestier, N., Marouan, A., Dib, M., Meininger, V., 2002. Glutamate levels in cerebrospinal fluid in amyotrophic lateral sclerosis: a reappraisal using a new HPLC method with coulometric detection in a large cohort of patients. J. Neurol. Sci. 193, 73–78.

Stobart, J.L., Lu, L., Anderson, H.D., Mori, H., Anderson, C.M., 2013. Astrocyte-induced cortical vasodilation is mediated by D-serine and endothelial nitric oxide synthase. Proc. Natl. Acad. Sci. U. S. A. 110, 3149–3154.

Su, X.W., Broach, J.R., Connor, J.R., Gerhard, G.S., Simmons, Z., 2014. Genetic heterogeneity of amyotrophic lateral sclerosis: implications for clinical practice and research. Muscle Nerve 49, 786–803.

Swarup, V., Phaneuf, D., Dupré, N., Petri, S., Strong, M., Kriz, J., Julien, J.-P., 2011. Deregulation of TDP-43 in amyotrophic lateral sclerosis triggers nuclear factor κB–mediated pathogenic pathways. J. Exp. Med. 208, 2429–2447.

Tai, L.M., Reddy, P.S., Lopez-Ramirez, M.A., Davies, H.A., Male, D.K., Loughlin, A.J., Romero, I.A., 2009. Polarized P-glycoprotein expression by the immortalised human brain endothelial cell line, hCMEC/D3, restricts apical-to-basolateral permeability to rhodamine 123. Brain Res. 1292, 14–24.

Teichberg, V.I., Cohen-Kashi-Malina, K., Cooper, I., Zlotnik, A., 2009. Homeostasis of glutamate in brain fluids: an accelerated brain-to-blood efflux of excess glutamate is produced by blood glutamate scavenging and offers protection from neuropathologies. Neuroscience 158, 301–308.

Tian, G.F., Azmi, H., Takano, T., Xu, Q., Peng, W., Lin, J., Oberheim, N., Lou, N., Wang, X., Zielke, H.R., Kang, J., Nedergaard, M., 2005. An astrocytic basis of epilepsy. Nat. Med. 11, 973–981.

Turini, M.E., DuBois, R.N., 2002. Cyclooxygenase-2: a therapeutic target. Annu. Rev. Med. 53, 35–57.

Ueda, Y., Tsuru, N., 1995. Simultaneous monitoring of the seizure-related changes in extracellular glutamate and gamma-aminobutyric acid concentration in bilateral hippocampi following development of amygdaloid kindling. Epilepsy Res. 20, 213–219.

van Vliet, E.A., Zibell, G., Pekcec, A., Schlichtiger, J., Edelbroek, P.M., Holtman, L., Aronica, E., Gorter, J.A., Potschka, H., 2010. COX-2 inhibition controls P-glycoprotein expression and promotes brain delivery of phenytoin in chronic epileptic rats. Neuropharmacology 58, 404–412.

Wilhelm, I., Fazakas, C., Krizbai, I.A., 2011. In vitro models of the blood-brain barrier. Acta Neurobiol. Exp. 71, 113–128.

Zhu, H.J., Liu, G.Q., 2004. Glutamate up-regulates P-glycoprotein expression in rat brain microvessel endothelial cells by an NMDA receptor-mediated mechanism. Life Sci. 75, 1313–1322.

Zibell, G., Unkruer, B., Pekcec, A., Hartz, A.M., Bauer, B., Miller, D.S., Potschka, H., 2009. Prevention of seizure-induced up-regulation of endothelial P-glycoprotein by COX-2 inhibition. Neuropharmacology 56, 849–855.